

ABSTRACT

Understanding the Effects of High Altitude Electromagnetic Pulse on the US Power Grid
by Creating a Power Grid Model and Analyzing Transformer Susceptibility

David A. Ridley, M.S.E.C.E.

Supervising Professor: W. Mack Grady, Ph.D.

The purpose of this thesis is to address two topics in understanding the effects of high altitude electromagnetic pulse (HEMP) E3 by determining the latitude and longitude of loadflow buses, and analyzing transformers as the largest risk. This paper will outline the methods used to create a geographic grid model based on the Texas grid. Latitude and longitude values were found for 5000 buses in a grid. Each pair of latitude and longitudes was taken and plotted using Google Earth to verify the locations. With this data a model for the grid was created for a HEMP simulation program. This paper will also cover the analysis of a high voltage (HV) transformer during a HEMP E3 test. This provides an understanding of how harmonics created by HEMP E3 effect the transformer based on loading and the amount of geomagnetically induce current (GIC) into the transformer.

Understanding the Effects of High Altitude Electromagnetic Pulse on the US Power Grid by
Creating a Power Grid Model and Analyzing Transformer Susceptibility

by

David A. Ridley, B.S.E.C.E.

A Thesis

Approved by the Department of Electrical and Computer Engineering

Kwang Y. Lee, Ph.D., Chairperson

Submitted to the Graduate Faculty of
Baylor University in Partial Fulfillment of the
Requirements for the Degree
of

Master of Science in Electrical and Computer Engineering

Approved by the Thesis Committee

W. Mack Grady, Ph.D., Chairperson

Annette von Jouanne, Ph.D.

Byron Newberry, Ph.D.

Accepted by the Graduate School

May 2019

J. Larry Lyon, Ph.D., Dean

Copyright © 2019 by David A. Ridley

All rights reserved

TABLE OF CONTENTS

LIST OF FIGURES	v
ACKNOWLEDGMENTS	vii
DEDICATION	viii
CHAPTER ONE	1
Introduction.....	1
CHAPTER TWO	2
Background.....	2
2.1 <i>High-Altitude Electromagnetic Pulse Description</i>	2
2.2 <i>Geomagnetically Induced Currents from Space Weather</i>	4
CHAPTER THREE	6
Recreating a Power Grid.....	6
3.1 <i>A Power Grid</i>	6
3.2 <i>Creating the geographic model</i>	7
3.3 <i>Results</i>	13
CHAPTER FOUR.....	17
HEMP Test Data Analysis.....	17
4.1 <i>HEMP Test Background</i>	17
4.2 <i>Preparing the Test Data</i>	18
4.3 <i>Analyzing the Data</i>	20
4.4 <i>Analysis Results</i>	29
CHAPTER FIVE	33
Closing Remarks.....	33
5.1 <i>Future works</i>	33
5.2 <i>Conclusion</i>	33
BIBLIOGRAPHY.....	34

LIST OF FIGURES

Figure 1 - HEMP Components [1].....	2
Figure 2 – Starfish Prime Blast [2]	3
Figure 3 – Grid slice example.....	7
Figure 4 – Deciding if the shortest path from 1 to 5 is direct, (a.) through 4, or (b.) through 2. (Distances not to scale).....	8
Figure 5 – Ring 1 (a.) and Ring 2 (b.) of “Method of Rings”. The dotted lines represent imaginary connections while the solid represents actual wire connecting buses.	9
Figure 6 – Example of circle overlap to estimate bus location.....	11
Figure 7 – Code for Google Earth points and connections. The first “<placemark>” tag is the point and within the second is the line.....	12
Figure 8 – (a.) 345 kV grid model with 145 buses where 136 are known locations. (b.) 138 kV grid model with 2638 buses where 1513 are known locations. (c.) 69 kV grid model with 1890 buses where 1059 are known locations.....	13
Figure 9 – (a.) Example of an estimate that is 1 mile away from the actual location. (b.) Example of a reference location with the substation beneath the point.....	14
Figure 10 – Full Texas grid map.....	15
Figure 11 – Flowchart from getting the data to being able to use it	17
Figure 12 – Fourier file for use in other programs containing the values for Fourier coefficients for a 50ms window as well as the harmonic magnitudes and angles.....	19
Figure 13 – Fourier Recreation.....	20
Figure 14 – 1024 Point Recreation	20
Figure 15 – Quick reference pages. (a.) Voltage and Current, (b.) Harmonic Spectrums, (c.) Power, (d.) Time.....	24-27
Figure 16 – Test layout overview	28

Figure 17 – Phase A voltage harmonics for 50% complex and resistive load on the low side of a HV transformer with (a.) 32 A injection, (b.) 62 A injection, (c.) 92 A injection, (d.)122 A injection30

Figure 18 – Voltage waveforms for 50% complex and resistive load on a HV transformer (a.) 32 A injection, (b.) 62 A injection, (c.) 92 A injection, (d.)122 A injection.....31

Figure 19 - Dirty (a.) and Clean (b.) feed waveforms where additional harmonics are present in the clean feed.....32

ACKNOWLEDGMENTS

I would like to thank the Department of Defense and Defense Threat Reduction Agency for funding this research. I am especially grateful for Dr. W. Mack Grady and his guidance. The opportunity to work on this project has been invaluable experience. Lastly, I would like to thank my mother and father. I cannot thank them enough for their love and support.

DEDICATION

To Mom and Dad with love

CHAPTER ONE

Introduction

Nuclear weapons are a destructive force at both low and high altitudes. The threat is real, and it is best to be prepared for the worst when high loss of life is concerned. The effect of a high-altitude electromagnetic pulse (HEMP) has the potential to take down electrical systems in a massive region for months. HEMP is a threat to power grids on the large scale and down to cell phones on the small scale. Some damage may go unnoticed until it is too late and causes a catastrophe. The motivation behind this research is to understand how HEMP would affect a power grid in order to properly harden equipment in the event of an attack.

One benefit from understanding HEMP is the similar effects of solar flares. Geomagnetic disturbance (GMD) from severe space weather and HEMP E3 create geomagnetically induced currents (GIC) on long conductors. In this paper GMD will refer to the space weather disturbances as is convention. Sharing the research on HEMP with utilities can provide valuable information on hardening grids to potential damages from space weather.

CHAPTER TWO

Background

2.1 High-Altitude Electromagnetic Pulse Description

HEMP is the explosion of a nuclear weapon at altitudes of 60 km and above. The blast lasts for hundreds of seconds as it shifts between three forms over several minutes: E1, E2, and E3. Fig. 1 shows the various phases for HEMP and their time frame.

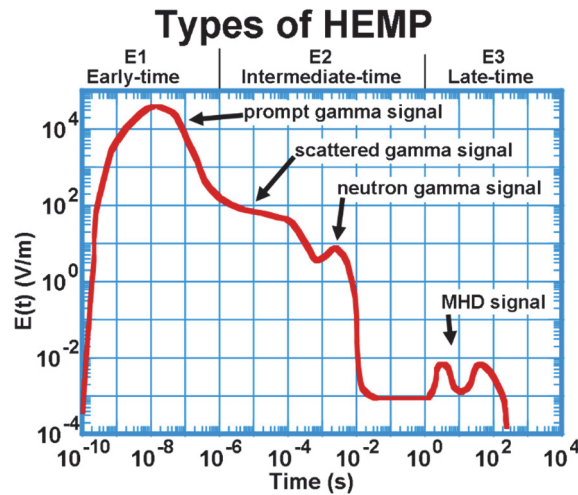


Figure 1 - HEMP Components [1]

E1 is the fast-acting component of a blast and can destroy electronics immediately. This is created by gamma radiation in the upper atmosphere stripping electrons that then combine with Earth's magnetic field to create a pulse of electromagnetic energy that travels at nearly the speed of light. An intense magnetic field is produced that creates high voltage in electrical conductors.

E2 is the second phase and is a slower pulse that lasts up to 1 second after the explosion. E2 is essentially an extension of E1 with lower magnitude. It can be protected against in the same fashion as lightning. The two are similar and electromagnetic pulses from nearby lightning strikes are often larger than the E2 component of HEMP. The concern comes from E1 damaging protection devices with no time for them to recover before E2 hits.

Finally, E3 is the slowest of the pulses and can last for hundreds of seconds. This pulse is created by the distortion and recreation of the Earth's magnetic field. GIC like a geomagnetic storm is created that can couple to long distance electrical conductors such as power or communication lines. A quasi-direct current (DC) is induced and is greatest in long transmission lines, with magnitudes reaching thousands of amperes. The area of effect of E3 is large enough to cover a significant portion of a continent in a single blast.

These pulses combine to create a terrible weapon that does not cause casualties directly but is, nevertheless, disastrous.

HEMP is a world of unknowns since very few tests have been done with the weapons. Many assumptions come from Operation Fishbowl in 1962 and only five tests were successful. The largest of which is known as Starfish Prime as seen in Fig. 2.



Figure 2 – Starfish Prime Blast [2]

Starfish Prime was a 1.4 megaton explosion about 250 miles above the Pacific Ocean about 900-miles from Hawaii where some effects of the blast were felt [3]. Streetlights went out, car alarms set off, a telecommunications company was downed, and even some low earth orbit satellites were disabled. Despite all this, very few data were recorded due to the blast being larger than expected, causing some instrumentation to go off the scales.

2.2 Geomagnetically Induced Currents from Space Weather

Many times a year the sun ejects coronal mass (CME) commonly known as solar flares. When solar activity is most active CME can happen two to three times a day. The high energy mass can disrupt the earth's geomagnetic field and create GIC in long transmission lines and transformers [1]. The created geomagnetic fields can last from a few seconds up to days and may not be noticed until weeks after the event.

The largest solar storm occurred in August and September of 1859 and is known as the Carrington Event. Technology's presence was only a fraction of what there is today. Most effects were noted in the telegraph system where operators reported that lines

would stop working or in some cases even caused electric shock [4]. This is an example of the high currents created on a long conductor such as power lines.

The next largest event occurred during the space age in March 1989 where the entire Quebec grid lost power for twelve hours and massive power losses occurred in the northeast states [5]. This solar storm is estimated to be one third the size of the Carrington Event. Greater advancements in technology did not help to protect equipment from the damage. As technology grows more complex it is likely that greater damage will occur.

With the similarities between E3 and GMD, many approaches to E3 hardening will also apply to GMD. Sharing data between these studies will help complete a picture of the necessary steps to prepare a grid for such events.

CHAPTER THREE

Recreating a Power Grid For HEMP Studies

3.1 A Power Grid

The US is divided into three power grids, the western grid, the eastern grid and the Texas grid. Several regions of the grid are operated by an independent system operator (ISO). The ISO in Texas is known as the Electric Reliability Council of Texas (ERCOT). DC ties connect each region of the US and allow some power to be transferred between grids. This is done through high voltage DC lines that effectively isolate the AC frequencies to either side.

A power grid is a complex balanced system where a large enough disruption can cause large region wide outages for undetermined amounts of time. An example is a natural disaster such as a hurricane where it can take weeks to get power back to all customers. However, HEMP is on a much more dangerous scale because it is the core components of the grid that would be damaged, opposed to power lines from a hurricane. Understanding how the damages of HEMP will propagate between substations is vital for recovery efforts. The Defense Threat Reduction Agency (DTRA) created the Electromagnetic Reliability and Effect Prediction (EMREP) program to estimate the amount of damage caused to a power grid from a nuclear device. While estimating how a weapon works is one challenge, creating an accurate model of a power grid is another altogether.

After the 9/11 attacks much of the electric utilities data has become confidential for fear of vulnerabilities being discovered. Data that predated 9/11 were publicly available and used in order to determine locations of older buses. These older buses are most likely still used since the power grid does not change rapidly. The data contained load-flow study parameters for the three voltage levels in Texas: 69 kV, 138 kV, and 345 kV. In a load-flow study, bus and line data are used to calculate the voltages, currents, and power flows in a grid during specific load conditions. The bus data contains real power and reactive power as well as voltage magnitude and angle. The line data contains bus connections and their lengths as well as resistance and impedance values.

3.2 Creating the Geographic Model

To begin modelling the locations it is important to have a strong list of reference bus locations to begin estimating the others. This is done through bus names and a familiarity with Texas. In a few cases some bus names correspond to the town or city they are in. Once a general area is identified, a map of ERCOT transmission from 2009 is then used to narrow down the location. As an example, consider a bus named “138MASON” with bus number 39. It is safe to assume the bus is connected to the 138 kV network and possibly in the area of Mason, Texas. From there Mason is located on the 2009 map as shown in Fig. 3. The blue lines represent the 138 kV network, attached to which is bus number 39, but with a different name. Different names are common for many buses, as names change or are repeated throughout the state. However, bus number is usually unchanged. The example bus is shown to be northeast of the city, which can be used in Google Earth to visually confirm a substation with exact latitude and longitude.

This process was repeated for approximately 100 locations with easily identifiable names in order to start a list of references.

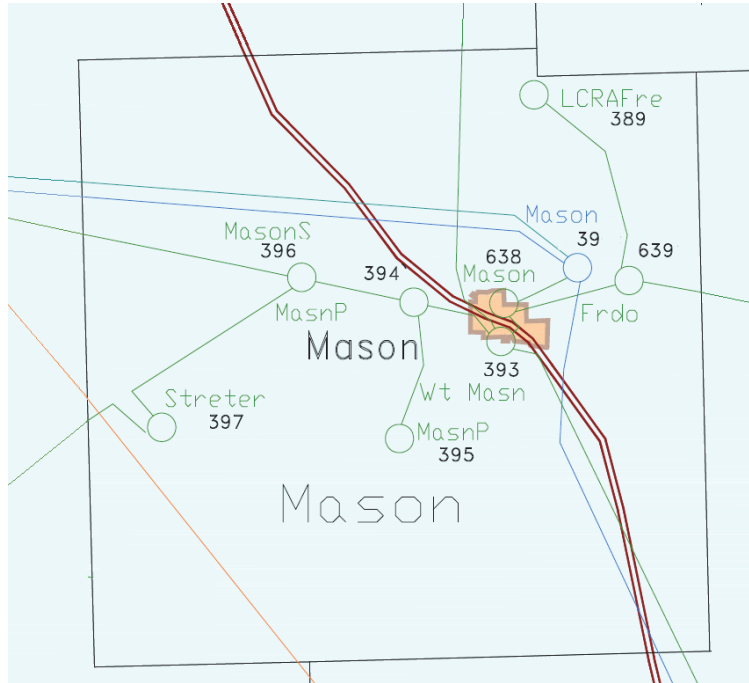


Figure 3 – Grid slice example

Method of Rings

Once the 100 reference buses were found with reasonable confidence it was then possible to estimate other bus locations using the “Method of Rings”. This is a developed method that uses distances between buses to calculate how far a bus is from every other bus. Within the line data, distances are included for the length of many connections. If the length is not provided it can be calculated using the impedances of the line. The line lengths represent the actual wire distance between buses. The shortest wire path represents the maximum geographical distance between buses, because the connection between two buses is not always a straight line and may curve to bypass an obstacle. The

“Method of Rings” finds the shortest wire path between buses using the available distances

To begin, the “Method of Rings” picks a bus that is not in the list of references. The connections it has are known. The connected buses are known as the ring of neighbors. It looks at all the distances to find the shortest wire path between buses. The direct path may not be the shortest so the indirect distances through neighboring buses are calculated until the shortest wire path is found. Fig. 4 shows an example of how the shortest path from 1 to 5 may be through 2 or 4.

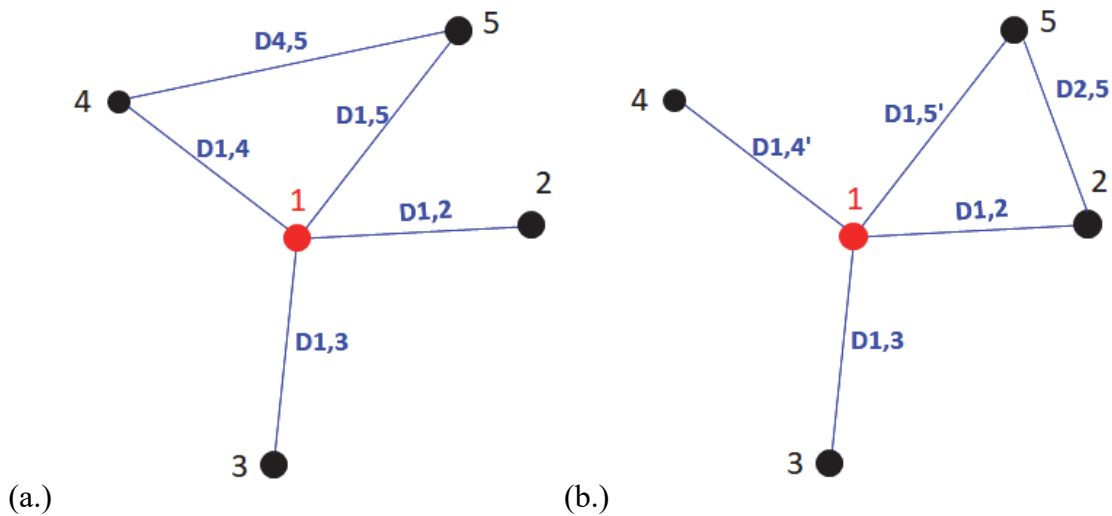


Figure 4 – Deciding if the shortest path from 1 to 5 is direct, (a.) through 4, or (b.) through 2.

Once the distances have been found the next ring of neighbors is added to the calculations. Fig. 5 shows the first ring compared to the second ring. More rings of neighbors are added leading to more possibilities for shortest path. Rings are added until

the distances from the first bus to every other bus is known. This then repeated to find the distances from every reference bus to every bus in the network.

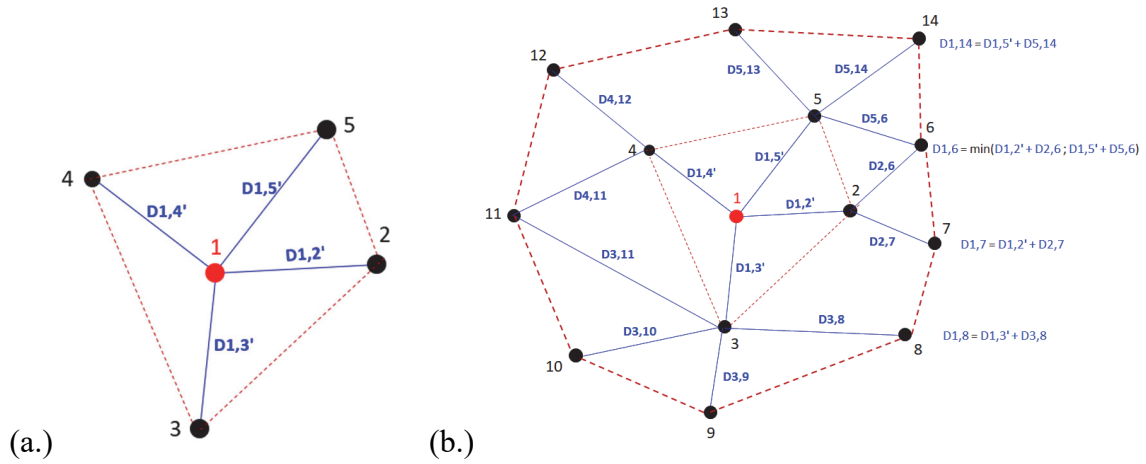


Figure 5 – Ring 1 (a.) and Ring 2 (b.) of “Method of Rings”. The dotted lines represent imaginary connections while the solid represents actual wire connecting buses.

The distances are used to estimate the buses without locations; referred to as unknowns. Circles centered at each reference point with the distance to an unknown as the radii are drawn. Where these circles overlap is the area where the unknown is most likely located as shown in Fig. 6.

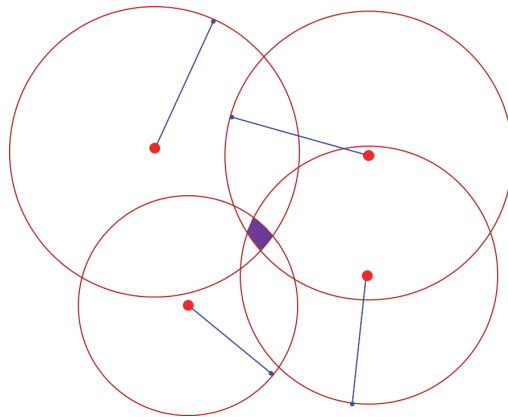


Figure 6 – Example of circle overlap to estimate bus location.

Google Earth Visual Confirmation

When estimated locations for all buses were found, confirmation is necessary to maximize accuracy. At first, locations were simply plotted on Google Earth using the bus number for reference. Strange behavior, such as points being in a straight line or resembling a circle, was noticed and used to improve the estimation procedure. As errors became less obvious more detail was required to assess locations. The connection data is where the next step of analysis was based. With the connection data included, the distance between two connected locations could be calculated using (1), where x represents latitude and y represents longitude for the points of interest. The constant R is the radius of the Earth.

$$Distance = \cos^{-1} (\sin x_1 * \sin x_2 + \cos x_1 * \cos x_2 * \cos(y_1 - y_2)) * R \quad (1)$$

Using distances, many incorrect estimates were identified. For example, a 1000 mile long connection for 69 kV buses means one of the locations is obviously impossible. Higher voltages lines are longer than lower voltages. The longest 345 kV line in the grid model is approximately 160 miles, the longest 138 kV line is about 60 miles, and the longest 69 kV line is about 50 miles. If one bus had only one connection it was taken and given a correct location using the 2009 transmission map method mentioned earlier. Once the location is known, it is then added to the reference bus list.

It became necessary as distances became smaller to plot all buses together and see what stood out visually from the whole picture. To do this a code was written to create Google Earth maps for each voltage level where bus name and number would be identified as points. The code language is known as Keyhole Markup Language (KML) and is the default for Google Earth [7]. The connections would then be added as straight

lines between two connecting points and labeled as such. The code needed to create each point and line can be seen in Fig. 7. The code allows for many details to be incorporated into each point. In this case only number, name, latitude, and longitude are shown, but any other information could also be added to the point description. Color was another customization option and light blue was chosen for an estimated point since it easily stood out from the rest even when zoomed out. Once this format was determined it was easily repeatable for all the buses in the case.

```

<name> TO EAGLE Known </name>
<Placemark>
  <name>EAGLE Known </name>
  <styleUrl>#msn_placemark_circle</styleUrl>
  <ExtendedData>
    <SchemaData schemaUrl="Info">
      <SimpleData name="Bus">100 </SimpleData>
      <SimpleData name="Name">EAGLE </SimpleData>
      <SimpleData name="Lat">32.29</SimpleData>
      <SimpleData name="Long">-97.64</SimpleData>
    </SchemaData>
  </ExtendedData>
  <Point>
    <coordinates>-97.64,32.29</coordinates>
  </Point>
</Placemark>
<Placemark>
  <name>ALLI Unknown Connected to EAGLE Known </name>
  <styleUrl>#pointStyleMap0</styleUrl>
  <LineString>
    <tessellate>1</tessellate>
    <coordinates>-97.64,32.29 -97.30,33.08</coordinates>
  </LineString>
</Placemark>

```

Figure 7 – Code for Google Earth points and connections. The first “<placemark>” tag is the point and within the second is the line

These maps were created for three voltage levels: 345 kV, 138 kV, and 69 kV.

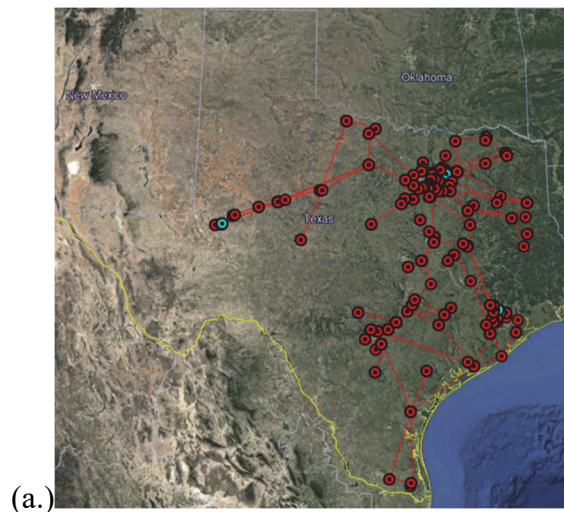
Focus was given to the 345 kV network since it had the fewest number of buses and

faced the largest threat from E3. Some estimates that stood out were listed and then compared to the 2009 map so they could be added as reference points.

3.3 Results

Using the “Method of Rings” and Google Earth for confirmation, the Baylor grid model found locations for approximately 4700 buses where 58% were considered to be reference locations with reasonable confidence. Approximately 5000 connections link the buses together into the grid model. Fig. 8 shows the three voltage levels of the model. The estimated points are highlighted in a light blue to be easily identifiable when an error is apparent.

The ability to select any point on the map and zoom in to confirm that there is at least a substation within the vicinity is a huge advantage of Google Earth. An example of an estimate is seen in Fig. 9(a). This light blue estimate is just over a mile away from the actual location, a large power plant located in north Texas. The location of the earlier reference point, 138MASON can be seen in Fig. 9(b) where the substation is clearly right beneath the mark.



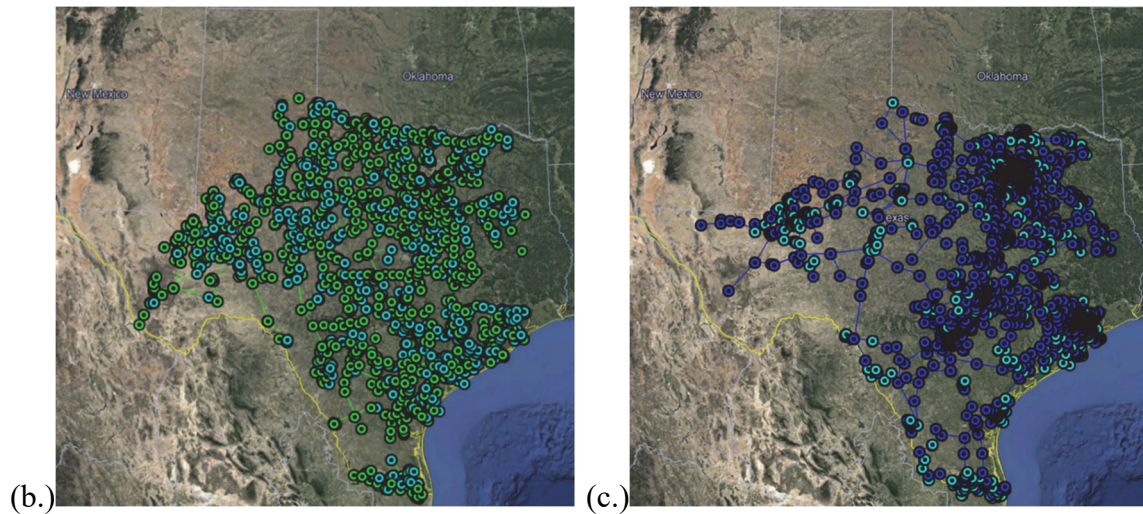


Figure 8 – (a.) 345-kV grid model with 145 buses where 136 are known locations. (b.) 138-kV grid model with 2638 buses where 1513 are known locations. (c.) 69-kV grid model with 1890 buses where 1059 are known locations.

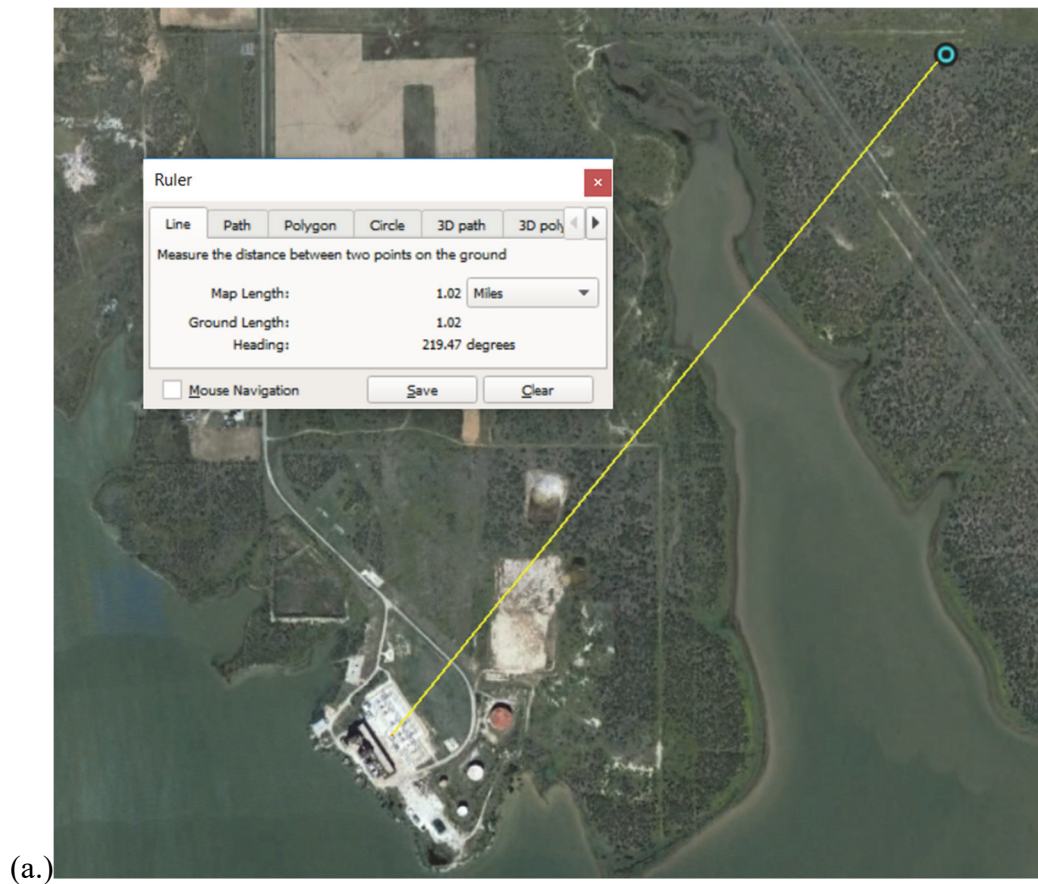




Figure 9 – (a.) Example of an estimate that is 1 mile away from the actual location. (b.) Example of a reference location with the substation beneath the point

All three grids come together to create the geographical map of the Texas grid as seen in Fig. 10, where more than half the buses are confirmed. This grid will be improved on with the hope of being incorporated into the EMREP software

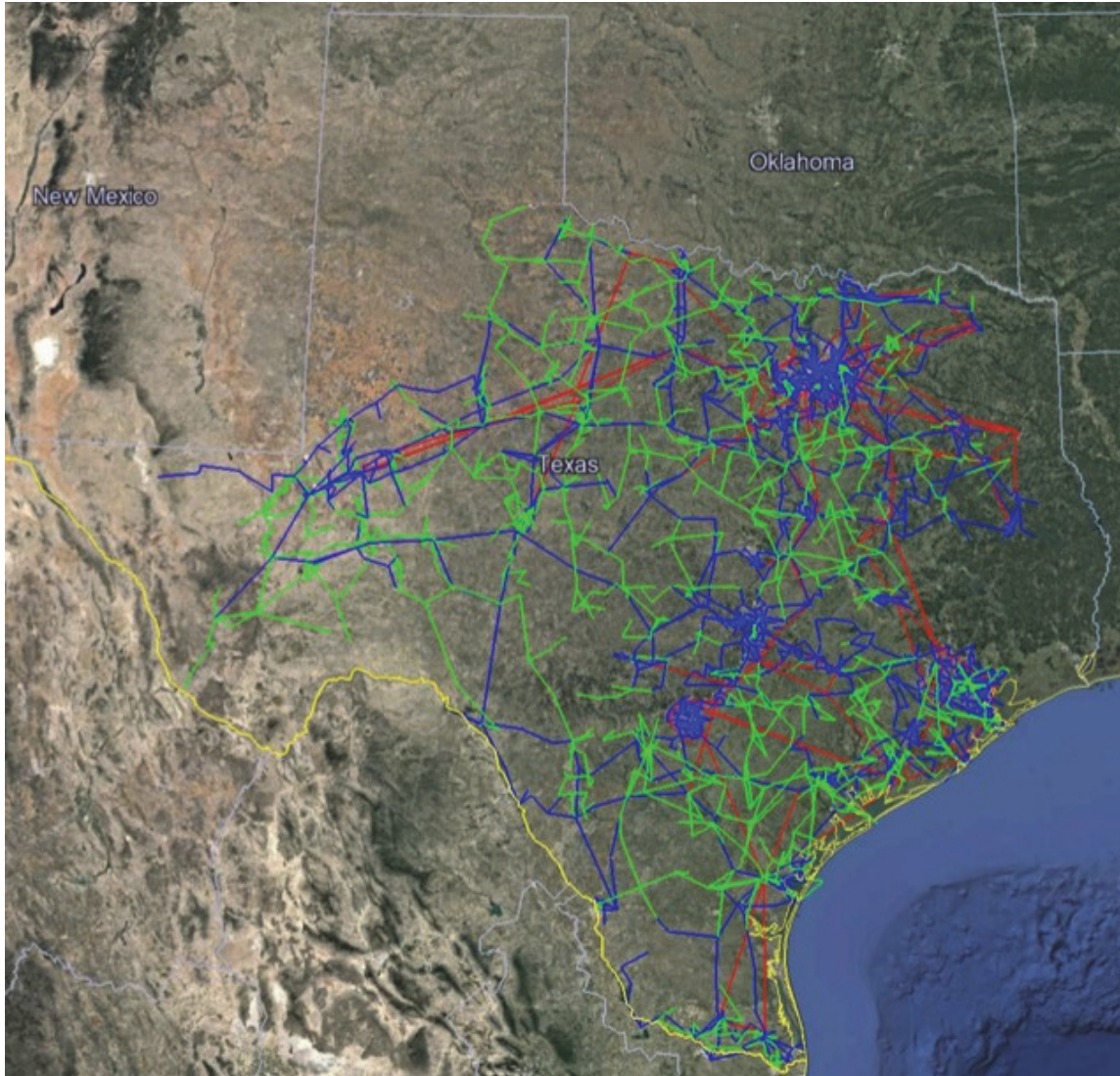


Figure 10 – Full recreated Texas grid map

CHAPTER FOUR

HEMP Test Data Analysis

4.1 HEMP Test Background

DTRA shared data from a substation equipment and loads HEMP test where DC was injected to the neutrals of two high voltage (HV) transformers. The injection was to mimic the quasi-DC of GIC using a set of 12 V batteries. Due to harmonic distortion created by HEMP, transformers are a major concern, especially with how vital they are in transferring electricity. The test was conducted on a 13 mile segment of an actual 138 kV grid. The goals of the test were to explore the primary and secondary threats of E3 while demonstrating the safety and test techniques required for E3 testing on a real piece of grid. The response, harmonic production, and operational responses from transformers and loads were analyzed to create a picture of the impacts of E3. The two transformers represented aging equipment that are commonly used in a power grid. One transformer was connected to resistive and complex loads to represent how actual load would react to GIC. With days of data during the testing from many measurement devices, some effects of HEMP can be inferred.

A total of 104 tests were conducted where the load and the amount of DC injection were varied. Each test lasted approximately 10 seconds and data was captured at a 100 kHz sampling rate. The first set of tests focused on purely resistive load at 10% and 50% of the transformer rating. The second set of tests were resistive and complex loading

at 10%, 50%, and 100% of the transformer rating. Each load was tested with DC injection levels ranging from 2 A to 122 A. There were approximately 126 measurement points per test and some of which did not always have useful data such as a case where what was being monitored was not energized for that test.

Large HV transformers were focused on for testing since they are what connect the power grid together. Many points from generation to customer voltages are stepped up and down with the help of transformers. With the loss of transformers from E3 much of the grid could fail. These large and expensive pieces of equipment are not easily replaced, because delivery can take up to 3 years. Roughly 100 transformers are produced in a year and distributed all around the world. Very little production of the HV transformers is done domestically. The EMP Commission notes that many newer substations are relying on three single phase transformers rather than a single three phase one due to the size and cost of three phase transformers [8]. Three phase systems are more resistant to GIC due to their balanced operation. Large GIC impacts transformers by pushing them into saturation which creates large harmonics. If many were to fail in a large region, the odds of having enough spare transformers to replace damaged ones is unlikely.

4.2 Preparing the Test Data

The data from the testing contained valuable information that required a detailed analysis. The process, from exporting the data to finally producing an easy to read quick reference, is shown in Fig. 11. Each step will be covered in this discussion.

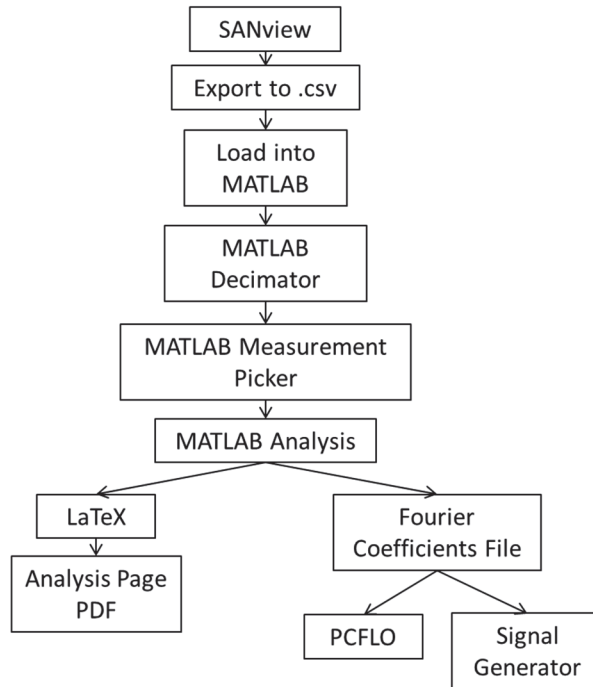


Figure 11 – Flowchart from getting the data to being able to use it.

Export to CSV Files

The data was originally formatted to work in one program called SANview, so it was important to convert to a format that was easy to work with in several existing programs for different analyses. Comma separated values (CSV) was chosen as the format and files were created for all 104 tests using the SANview export function.

MATLAB Decimation

The original 100 kHz sampling rate for 30 seconds of data led to extremely large files that were too big for many programs to open. 10 second samples were taken out of the data for the first analysis. During this, it was realized that for the purposes of this research, much of the high frequency data provided little to justify the large file sizes.

The decision to down sample the data to 20 kHz was made. This was done by loading the full data into MATLAB and taking every 50 μ s point.

MATLAB Measurement Selection

As previously mentioned, there were 126 separate measurements for all 104 tests conducted, and names for each were not always consistent. Some measurements also correspond to other points as well. For example, the data provided the input current for the HV transformers, but the voltage values were chosen from further upstream at the entrance to the testing station. Since a measurement is often inspected for each of the tests, a MATLAB code was implemented to select only what the user is interested in consistently for each test.

4.3 Analyzing the Data

After all the data was prepared, an analysis could begin. This includes a detailed look at voltage, current, and power for the different loading configurations and DC injection levels.

Fourier Analysis

A Fourier analysis is the first step, where the Fourier coefficients are solved for using the Fourier Equations (2-5). Variables a and b represent the various coefficients where k is the harmonic order. The equation $f(w)$ represents the data at point L_1 . A 50 ms window is used which corresponds to three cycles of the AC waveform. The start of the window is then moved 16.67 ms ahead, or a single cycle. This rolling window allows for overlap in the calculated Fourier coefficients, which is helpful in confirming accuracy.

$$f(w) = a_0 + \sum_{k=1}^{\infty} \left(a_k \cos \frac{kw}{L} + b_k \sin \frac{kw}{L} \right) \quad (2)$$

$$a_0 = \frac{1}{L} \int_{L_1}^{L_2} f(w) dw \quad (3)$$

$$a_k = \frac{1}{L} \int_{L_1}^{L_2} f(w) \cos \left(\frac{kw}{L_2 - L_1} \right) dw \quad (4)$$

$$b_k = \frac{1}{L} \int_{L_1}^{L_2} f(w) \sin \left(\frac{kw}{L_2 - L_1} \right) dw \quad (5)$$

A Fourier series is created for every 50ms window and is output to a text file as seen in Fig. 12 for several uses. These uses include confirming the recreation is correct, increasing the number of data points in a single cycle, and for use in loadflow harmonic analysis.

```

:Case Title, Measurement
:S086, LoadTrailer---CleanFeed---480I#PhaseA
:Fourier Series Window Start, Window Stop
:Harmonic (k), ak, bk, Mag, Angle
0,0.000050,0.050050
0,-0.213867,0,0,0
1,-42.136454,-106.879898,114.886002,111.516399
2,0.465014,1.222236,1.307707,-69.170106
3,1.443154,-0.787306,1.643942,28.614465
4,0.254643,-1.197567,1.224340,77.995784
5,-1.094224,-2.635604,2.853723,112.546762
6,0.016667,-0.026171,0.031028,57.509744
7,-3.853924,-3.886991,5.473704,134.755250
8,-0.393749,-0.319977,0.507369,140.901209

```

Figure 12 – Fourier file for use in other programs containing the values for Fourier Coefficients for a 50 ms window as well as the harmonic magnitudes and angles.

One of these uses is to recreate the waveform to confirm the Fourier series is correct. Fig. 13 shows a comparison of the calculated Fourier wave and the real wave. There is solid agreement in both waves to prove the Fourier recreation works. In this example only a 25 term Fourier series was used. However, thanks to the ease of MATLAB it is possible for a user to input any number of terms. Using 25 terms was

found to be consistent for this research, as nothing was noticed above the 25th harmonic with a high enough magnitude to be of concern.

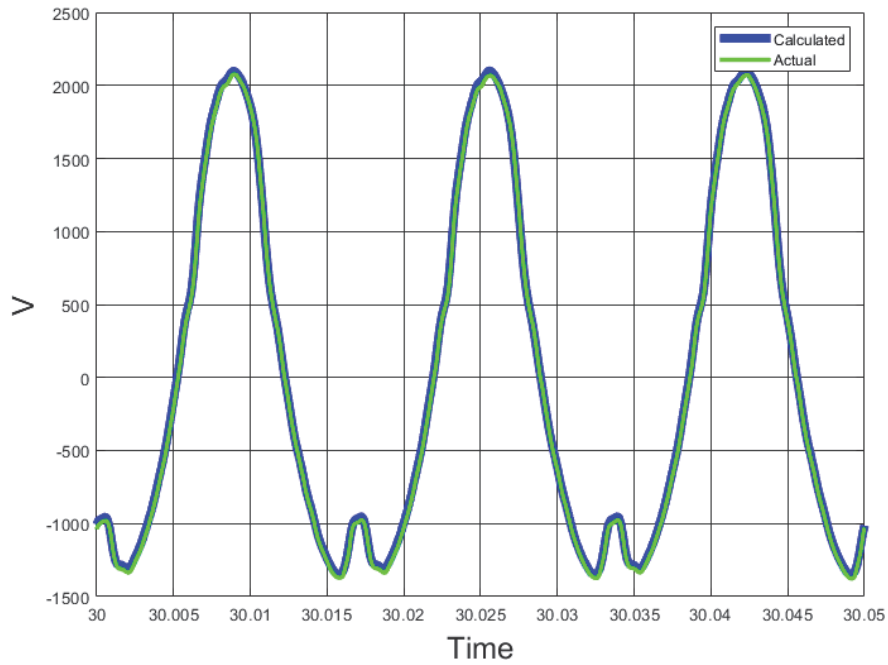


Figure 13 – Fourier comparison between calculated and actual

The next use was to recreate a single cycle that was increased to 1024 points. In the data a single cycle corresponds to approximately 333 points, so the data was adjusted to fit the window. The 1024 point recreation can be seen below in Fig. 13. The recreation has a good fit compared to the actual. This was used in a signal generator with the goal of replicating the events noticed in the HEMP test data on consumer electronics.

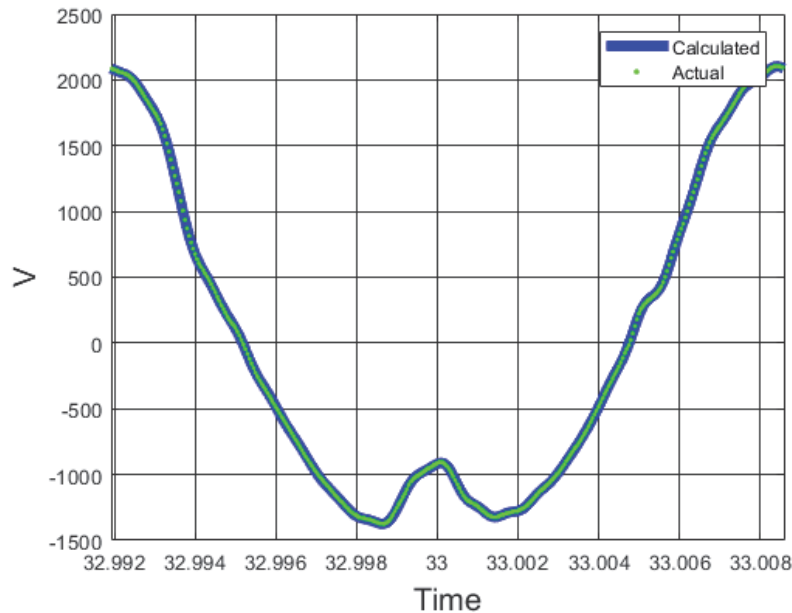


Figure 14 – 1024 Point Recreation

The final use for the 50 ms window recreation is for a program called PCFLO, written by Dr. W. Mack Grady for harmonic analysis on a loadflow grid. The harmonic magnitude and angles are used to simulate a scenario where a waveform existed in the grid with heavy harmonics.

Quick Reference Sets

With the large number of tests to look at, it was decided to create a quick reference set of 4 pages for every test that displayed various graphs of interest. The pages are consistent for every test and are ordered voltage, current, power, and time domain waveforms.

The first page, seen in Fig. 15(a.), starts with voltage RMS and is followed by RMSk, which is the sum of the higher order harmonics and how they impact the overall RMS, with the fundamental RMS following that. The last graph in the left column of

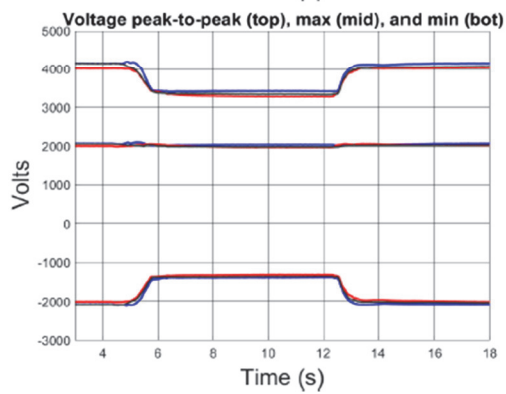
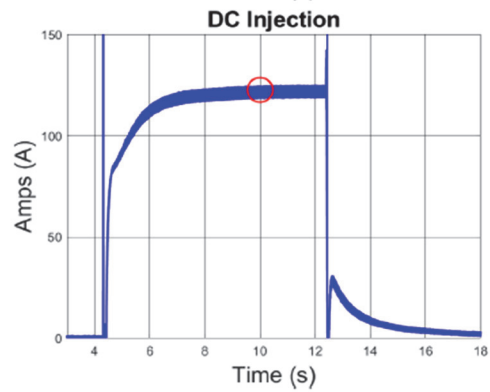
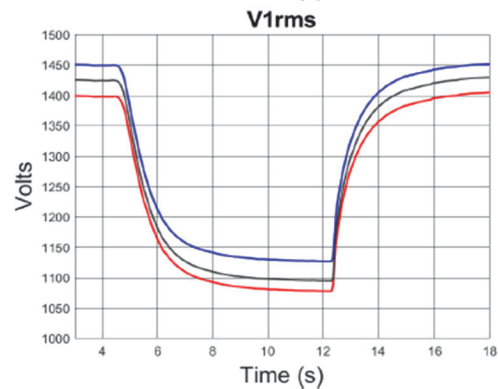
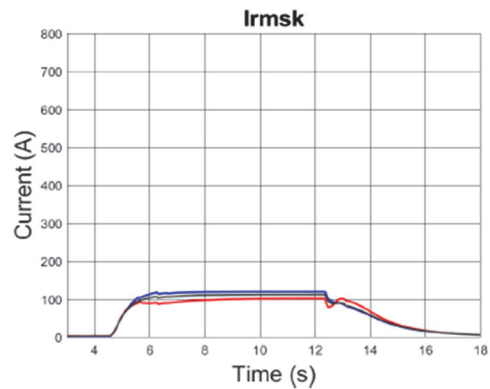
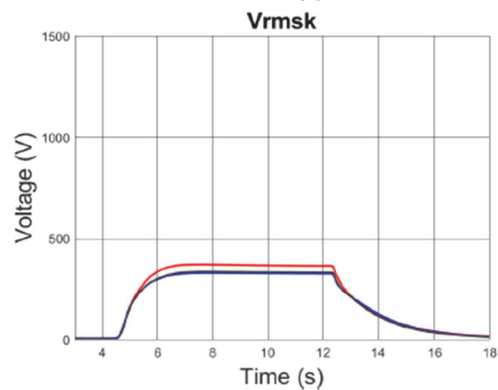
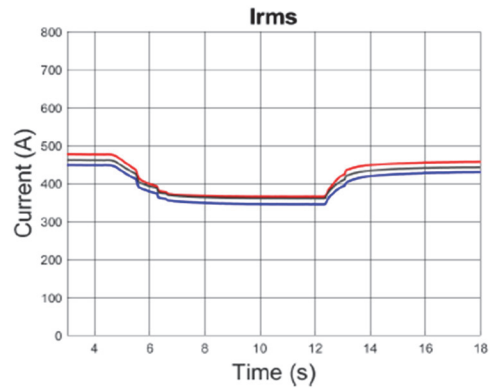
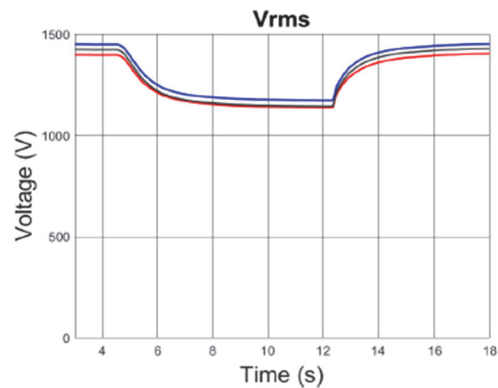
page one is the voltage peak-to-peak, maximum, and minimum, which is useful for determining overvoltage. The right column of page one is for current RMS and RMSk, followed by the plot of the injection current. The red circle indicates the time where the “during injection” analysis is conducted.

The second page, seen in Fig. 15(b.), contains the harmonic magnitudes for each phase voltage in the left column and current in the right column. These graphs were created using the harmonic magnitude values from the Fourier equations. Only the second through seventh harmonic can be seen on these graphs since it quickly becomes cluttered with many higher order harmonics plotted, or dwarfed if the fundamental is plotted.

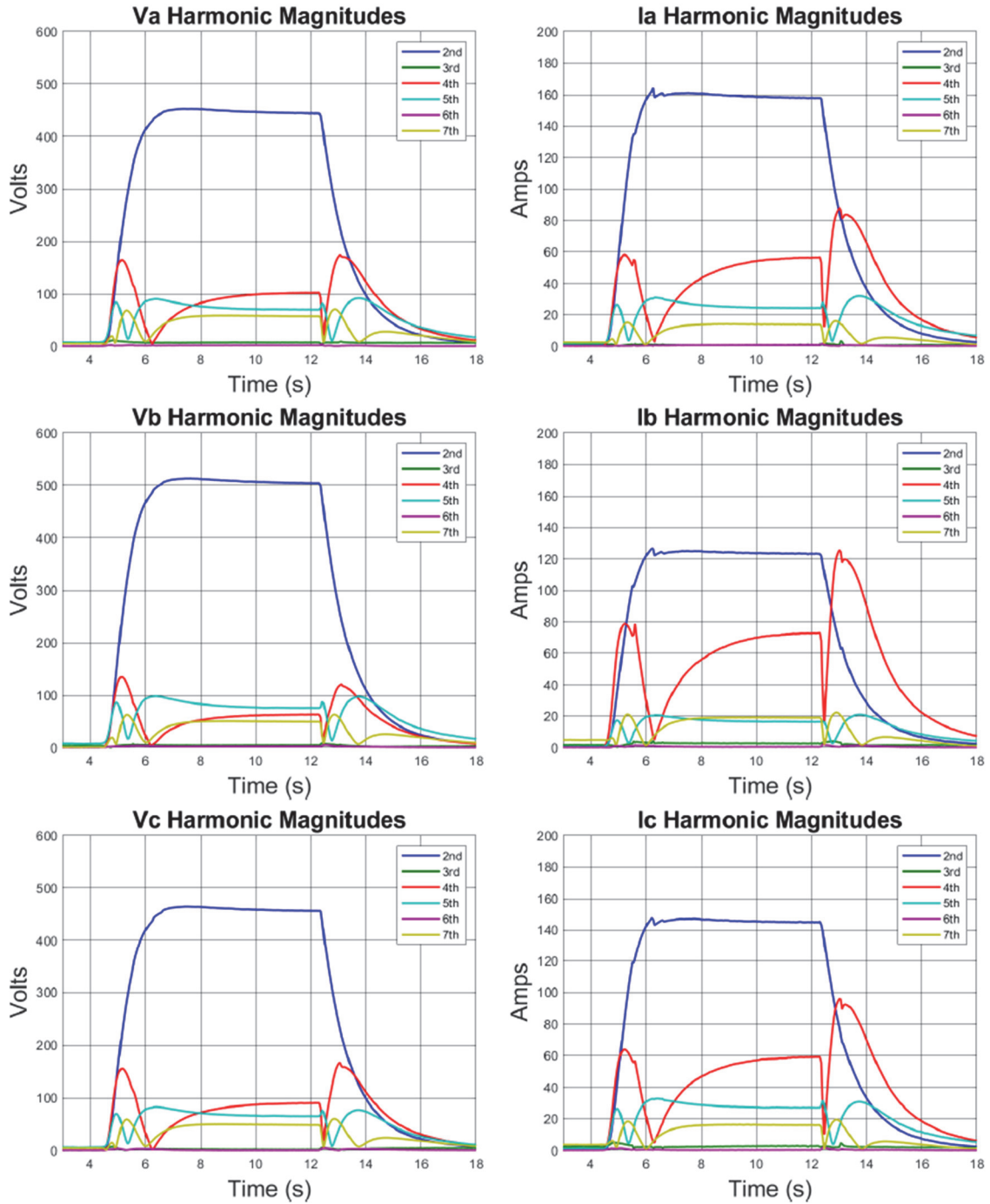
The third page seen in Fig. 15(c.) focuses on the power calculated from the voltage and current values in the data. The left column contains the average power per phase followed by the average three phase power, with the final graph being a plot of the maximum and minimum instantaneous power values taken in three cycle windows. The right column shows the power harmonic magnitudes that come from the Fourier series power calculation.

The fourth page, seen in Fig. 15(d.), shows the time domain views of the real waveforms. It was important to look at the waveform before, during, and after injection. The “before” plots confirm that the components are functioning normally during regular operation. Next, the “during” plots show how the waveform distorts due to DC injection and this is time marked by the red circle in the first page injection plot. Lastly, the “after” plots show how the waveform recovered once injection was turned off.

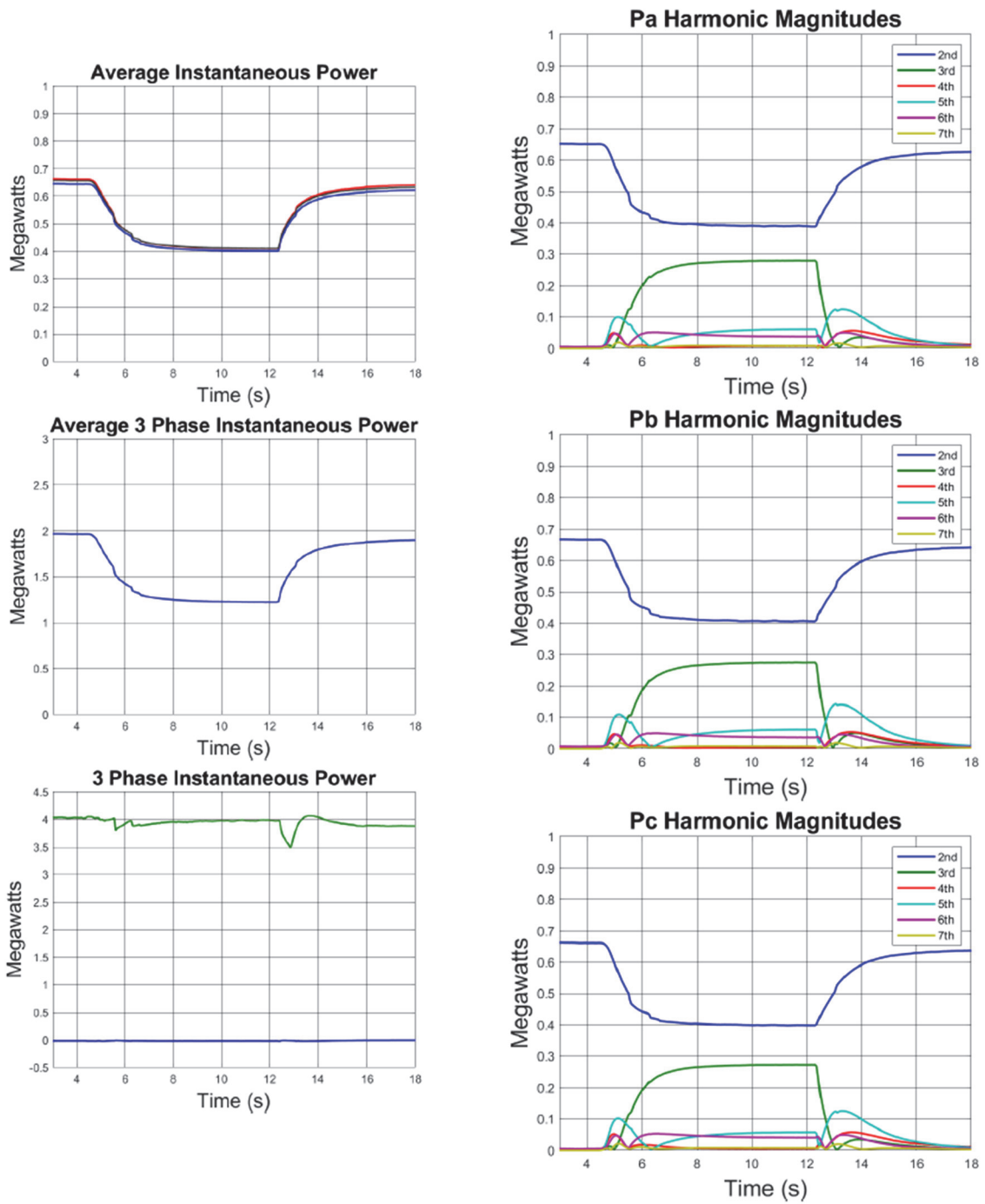
S062-0914-L5E-61-WestSecondary (50% Complex and Resistive Load)



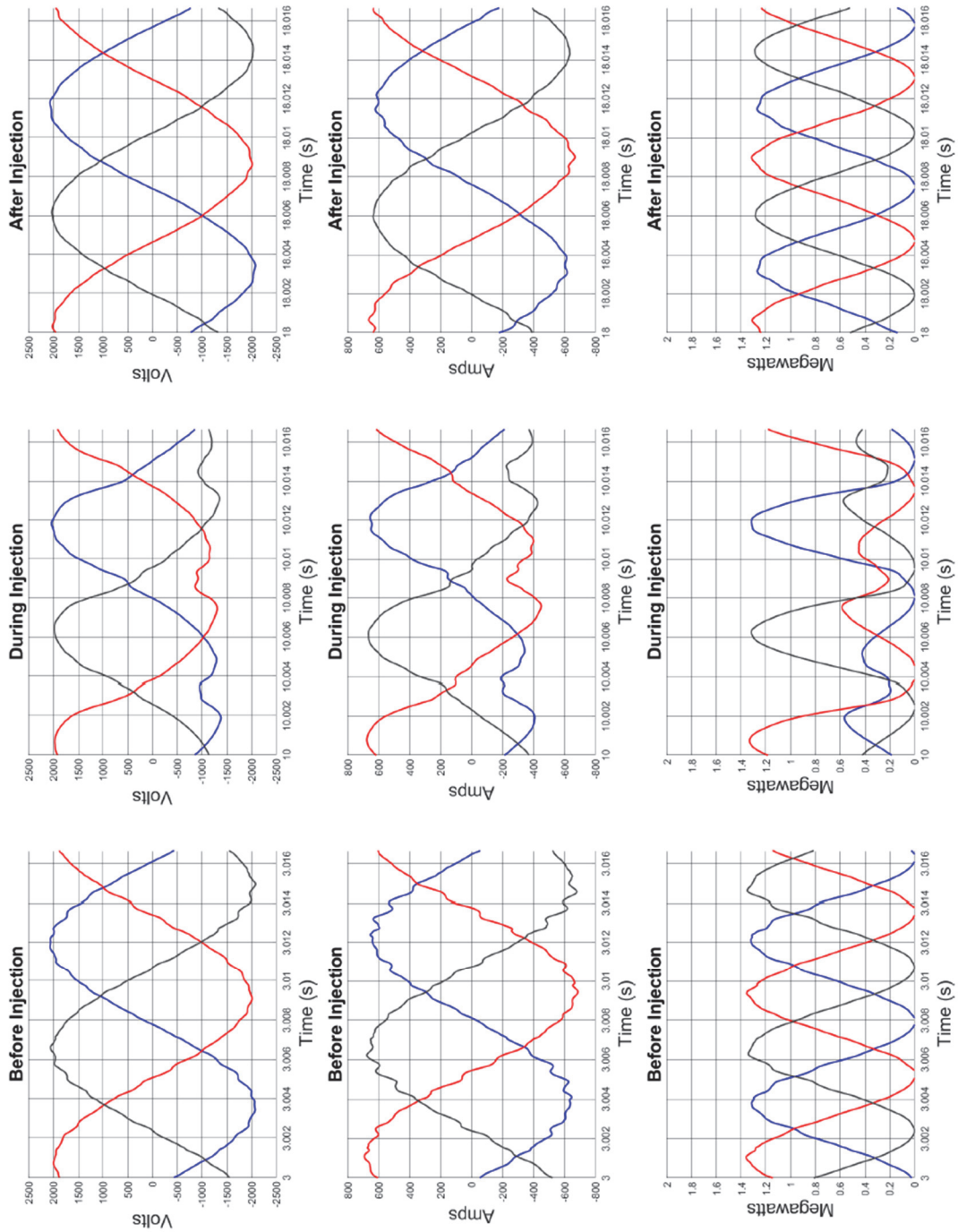
(a.)



(b.)



(c.)



(d.)

Figure 15 – Quick reference pages. (a.) Voltage and Current, (b.) Harmonic Spectrums, (c.) Power, (d.) Time Domain

4.4 Analysis Results

The focus of this analysis was downstream of the HV transformer that connected to the load. Fig. 16 shows the layout for the area of interest for this analysis. The analysis began with an interest in the way the load affected the harmonic spectrum.

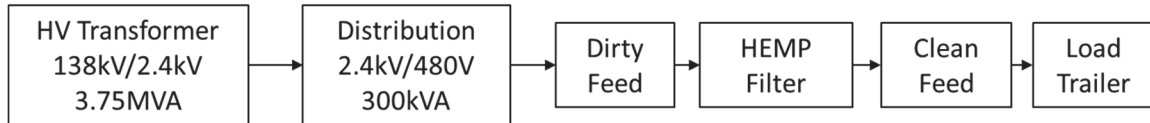


Figure 16 – Test layout overview

Fig. 17 shows the A phase voltage harmonics for different levels of injection on the low side of the HV transformer. Under different loading condition the same pattern appears as the injection current increases. It was determined from this that loading has very little effect on how much the transformer saturates. One area of interest found from this analysis is the sustained harmonic magnitudes of lower injection levels. In the 62 A injection case the fourth harmonic stays at a mostly constant magnitude for the duration of testing and is even greater than the magnitude of the 61 A case. Sustained higher order harmonics have potential to cause similar damage as lower harmonics at higher magnitudes.

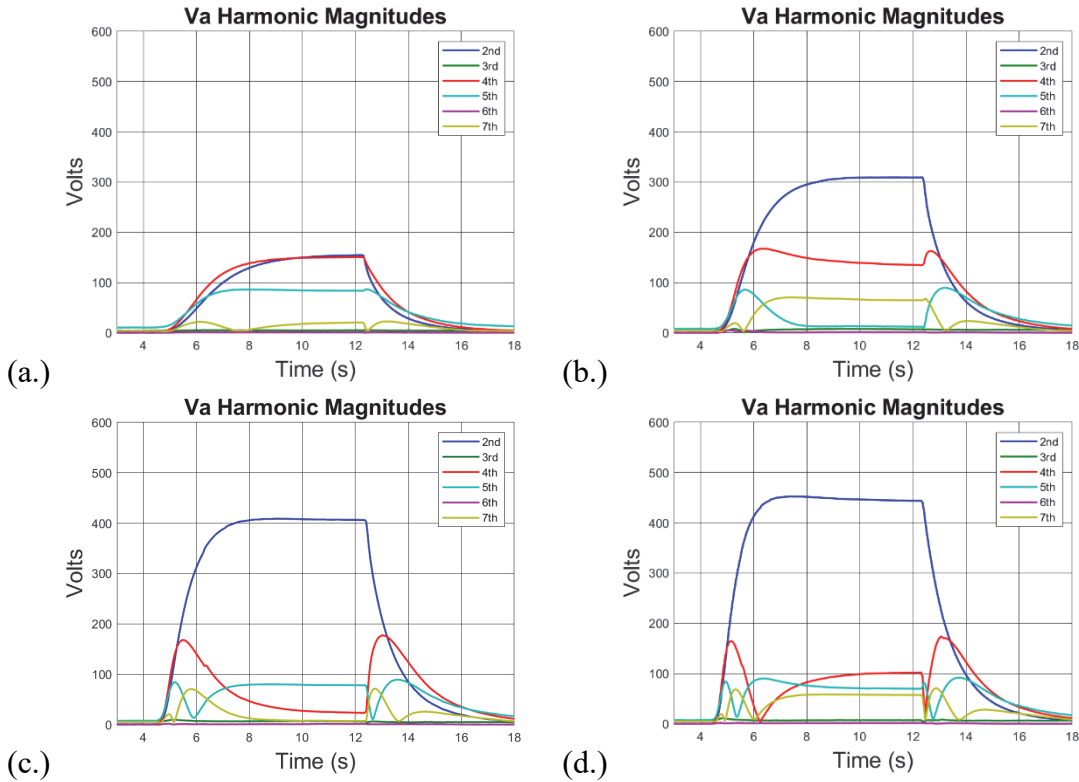


Figure 17 – Phase A voltage harmonics for 50% complex and resistive load on the low side of a HV transformer with (a.) 32 A injection, (b.) 62 A injection, (c.) 92 A injection, (d.)122 A injection

The effect of this pattern can be seen in the time domain waveforms during testing. The waveforms in Fig. 18 demonstrate the different outputs of the transformer based on the amount of DC injection. At low injections the half cycle peaks of the wave thinned as injection increased until a sharp point at the peak is created. As injection increases further the peak inverts and becomes a dip causing an asymmetric wave with a high peak of 2 kV and a low of -1.5 kV. The highest injection also experiences all the lower injection waveforms, just for much shorter durations, often one or two cycles only.

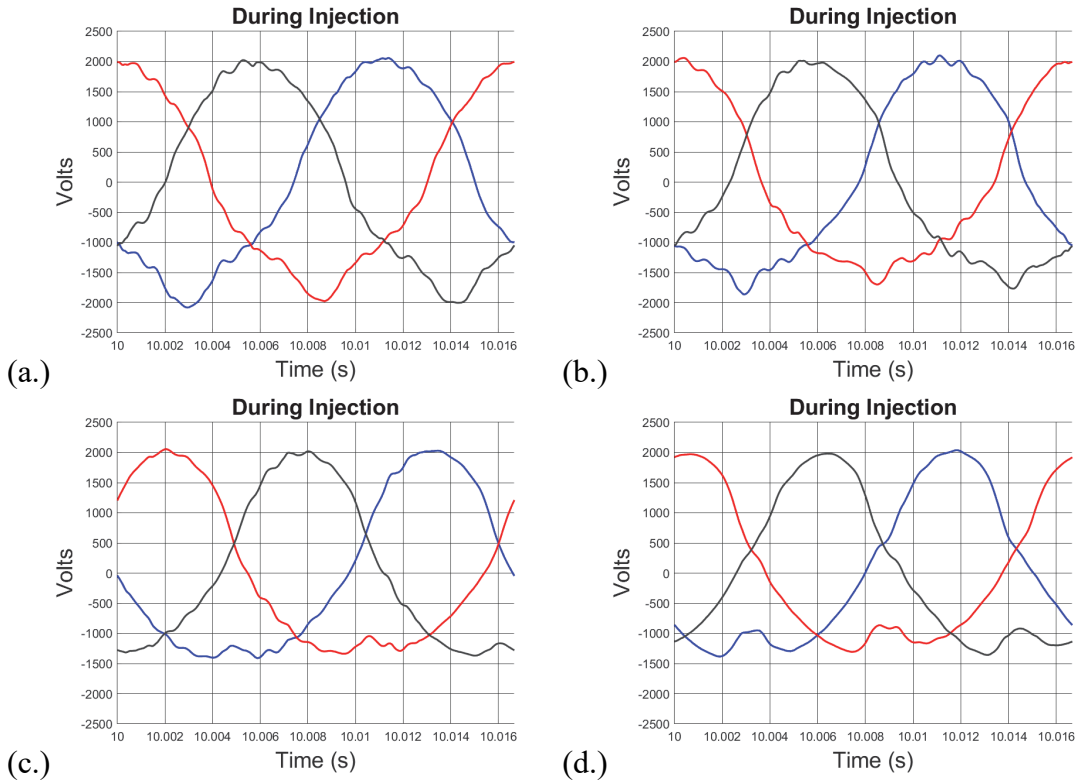


Figure 18 – Voltage waveforms for 50% complex and resistive load on a HV transformer (a.) 32 A injection, (b.) 62 A injection, (c.) 92 A injection, (d.) 122 A injection

A difference was noticed in the waveforms based on whether the loading was complex or purely resistive, and not based on the overall percentage load of the transformer. Due to complex loading, additional harmonic content was ringing within the load and was seen by the HEMP filter. The noisy “dirty feed” can be seen in Fig. 19.

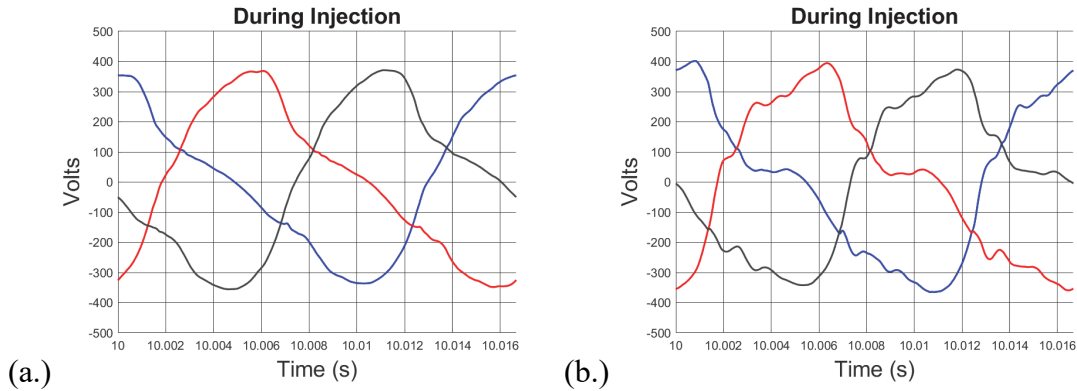


Figure 19 – Dirty (a.) and Clean (b.) feed waveforms where additional harmonics are present in the clean feed

Two set of tests were chosen as benchmark cases based on the analysis. These benchmark tests fall to two loading groups: 50% purely resistive load and 50% complex and resistive load. Since loading does not have a noticeable effect on the harmonic magnitudes, the higher loading was chosen. Within these two sets of four different injection levels were chosen: 32 A, 62 A, 92 A, and 122 A. Lower levels of injection showed very little activity and were excluded.

During the analysis some inconsistencies in the data were noticed. For instance, some current values were flipped so they were 180 degrees out of phase with the voltage. One larger issue was higher power coming out of the higher voltage transformer than what was going in. Fortunately, two other redundant measurement devices were located on the high side of the transformer to confirm the data. Since the problem did not appear to be on the high side it was determined that the low side would need to be adjusted. Voltage RMS values were consistent while current values seemed large. Current was then factored down based on the rating of the transformer.

CHAPTER FIVE

Closing Remarks

5.1 Future Works

The geographical model will continue to be fine-tuned as more of the buses become reference locations before being incorporated into EMREP. Each bus will need to be analyzed to find the grounding resistances at each bus and incorporate a grounding grid network that can be used for the calculation of GIC.

The continued analysis of the HEMP test data with the help of the created quick reference pages will create a better picture of how HEMP affects transformers and loads. Understanding the power transfer is the next area of interest for quick reference pages to understand how and where power losses are occurring. The Fourier recreation will be used within PCFLO to simulate how the grid would react to an actual waveform example. The single cycle recreations are to be used in testing of real world equipment provided by DTRA to determine how E3 affects customer products.

5.2 Conclusion

In conclusion HEMP E3 is a growing concern for a power grid. Little is known about how the grid will react if an event were to happen, but much can be learned from looking at GMDs effects in history. With a thorough analysis of test data and a real grid model, proper understanding of how these events will play out can be determined.

BIBLIOGRAPHY

- [1] J. Gilbert, J. Kappenman, W. Radasky, E. Savage. (2010 January). *The Late-Time (E3) High-Altitude Electromagnetic Pulse (HEMP) and Its Impact on the U.S. Power Grid*. Metatech Corporation. Goleta, California. [Online] Available: http://www.futurescience.com/emp/ferc_Meta-R-321.pdf
- [2] Sublette, C. (2005). *Operation Dominic*. [online] Nuclearweaponarchive.org. Available at: <http://nuclearweaponarchive.org/Usa/Tests/Dominic.html> [Accessed 24 Mar. 2019].
- [3] King, G. (2012). *Going Nuclear Over the Pacific*. [online] Smithsonian. Available at: <https://www.smithsonianmag.com/history/going-nuclear-over-the-pacific-24428997/> [Accessed 24 Mar. 2019].
- [4] Hathaway, D. H. (2014, August 14). Coronal Mass Ejections. Retrieved from <https://solarscience.msfc.nasa.gov/CMEs.shtml>
- [5] Boteler, D. H. "The Super Storms of August/September 1859 and Their Effects on the Telegraph System." *Advances in Space Research*, vol. 38, no. 2, 2006, pp. 159–172., doi:10.1016/j.asr.2006.01.013. [Accessed 7 Mar. 2019].
- [6] Dunbar, Brian. "The Day the Sun Brought Darkness." *NASA*, NASA, 13 May 2015, www.nasa.gov/topics/earth/features/sun_darkness.html.
- [7] "Keyhole Markup Language Google Developers," *Google*, 31-Oct-2018. [Online]. Available: <https://developers.google.com/kml/>. [Accessed: 24-Mar-2019].
- [8] EMP Commission. "Report of the Commission to Assess the Threat to the United States from Electromagnetic Pulse (EMP) Attack," [Online]. Available: [Accessed 3 Apr. 2019].
- D. H. Boteler and E. Bradley, "On the Interaction of Power Transformers and Geomagnetically Induced Currents," in *IEEE Transactions on Power Delivery*, vol. 31, no. 5, pp. 2188-2195, Oct. 2016.
- M. Shareghi, B. T. Phung, M. S. Naderi, T. R. Blackburn and E. Ambikairajah, "Effects of current and voltage harmonics on distribution transformer losses," 2012 IEEE International Conference on Condition Monitoring and Diagnosis, Bali, 2012, pp. 633-636.

- T. Dao and B. T. Phung, "Study of voltage harmonic effect on temperature rise in distribution transformer," 2016 IEEE International Conference on Power System Technology (POWERCON), Wollongong, NSW, 2016, pp. 1-5.
- T. Dao, H. A. Halim and B. T. Phung, "A comparative study of power loss caused by voltage harmonics in aged transformer," 2016 International Conference on Condition Monitoring and Diagnosis (CMD), Xi'an, 2016, pp. 461-464.
- Weisstein, Eric W. "Spherical Trigonometry." From MathWorld--A Wolfram Web Resource. <http://mathworld.wolfram.com/SphericalTrigonometry.html>